The Microwave Spectrum, Structure, and Internal Motion of the Cyclopropane-Water Complex

Anne M. Andrews, Kurt W. Hillig II, and Robert L. Kuczkowski*

Contribution from the Department of Chemistry, University of Michigan, Ann Arbor, Michigan 48109. *Received February 20, 1992*

Abstract: The microwave spectrum of the cyclopropane–water complex has been observed by Fourier-transform microwave spectroscopy. Only *a*-type transitions were observed; they were split into doublets of unequal intensity separated by 0.5–2 MHz. The stronger and weaker transitions were fit separately to rotational constants A = 19950 (100) MHz, B = 2518.845 (5) MHz, C = 2340.321 (5) MHz and A = 19945 (160) MHz, B = 2518.843 (7) MHz, C = 2340.876 (7) MHz, respectively. The water is hydrogen bonded to the center of an edge of the cyclopropane; the hydrogen bond is nearly linear (bond center–H–O angle = 180 (5)°) with the O and hydrogen-bonded H in the CCC plane. The hydrogen bond length (H-to-edge distance) is 2.34 Å. The position of the free H is uncertain. Nuclear spin statistics indicate that the splittings in the spectrum arise from a high-barrier internal motion of the water subunit which exchanges the two hydrogen atoms; a nearly free rotation of the water about the hydrogen bond is postulated to explain anomalous dipole moment and nuclear quadrupole coupling results. The μ_a dipole moment of the complex is determined as μ_a = 1.209 (10) D for the strong state and μ_a = 1.241 (10) D for the weak state. The nuclear quadrupole coupling constants for C_3H_6·HDO and C_3H_6·$H_2{}^{17}O$ were determined.

Introduction

Because intermolecular interactions involving water are important in many aspects of chemical, biological, and atmospheric sciences, water-containing molecular complexes have been the subject of a great deal of study.[1] Complexes of water with hydrocarbons such as ethylene and acetylene have been studied as models of hydrophobic interactions.[1a,b] The cyclopropane–water complex is of particular interest due to the anesthetic nature of cyclopropane. While it is widely accepted that anesthetic properties result from molecular associations, as opposed to chemical reactions, the nature of this interaction is not well understood. Relationships between lipid solubility and anesthetic potency have provided evidence that these interactions occur primarily in the lipid bilayer of the cell wall, but it has been proposed that polar interactions involving the interruption of hydrogen bonding by the anesthetic could be an important factor.[2]

In an ab initio study exploring this relationship, Hobza et al. sought the most stable structure of the cyclopropane–water dimer.[2] Their calculations put the water above the cyclopropane ring with the two planes perpendicular and the oxygen pointing toward the ring; this structure had an interaction energy of −2.88 kcal/mol. The cyclopropane–water complex has also been the subject of a matrix-isolation infrared spectroscopy study by Barnes and Paulson,[3] whose investigations suggested that both water hydrogens were involved in hydrogen bonding. Because the matrix IR experiment reveals only which bonds are affected by complexation, details of the structure were not determined, although a bifurcated structure with both hydrogens binding to a cyclopropane edge was proposed.

High-resolution gas-phase spectra have been observed by Fourier transform microwave spectroscopy for complexes of cyclopropane with HCl,[4] HF,[5] and HCN.[6] In each case, HX was hydrogen bonded to the center of a C–C bond, with the acid in the CCC plane. This is analogous to the structures of HX with ethylene[7] and acetylene[8] in so far as the pseudo-π system of cyclopropane is analogous to the π systems of ethylene and acetylene.[9] Similarly, complexes of ethylene, acetylene, and cyclopropane with sulfur dioxide all involve the S atom of the sulfur dioxide interacting with the π or pseudo-π system of the hydrocarbon.[10] The complexes of water with ethylene and acetylene have been studied using the molecular beam electric resonance technique by Peterson and Klemperer.[1a,b] Their studies revealed that while one hydrogen of the water was hydrogen bonded to the π system of the ethylene the acetylene was hydrogen bonded to the O atom of the water.

Considering these related studies, it was not obvious what model to choose to predict the spectrum of the gas-phase cyclopropane–water complex (C_3H_6·H_2O). Would the complex have a stacked-type structure as the ab initio study indicated (hereafter referred to simply as stacked), a bifurcated structure with two hydrogen bonds to a C–C edge as suggested by the matrix IR work (hereafter bifurcated), or would it be hydrogen bonded in the traditional sense as suggested by the cyclopropane–HX, ethylene–HX, and ethylene–water systems (hereafter hydrogen bonded)? Our microwave spectroscopic data provide evidence that the water forms a single hydrogen bond to a C–C edge with the oxygen in the CCC plane. Isotopic data suggest that the water undergoes a high-barrier internal motion interchanging the free and bonded hydrogens and a nearly free internal rotation about the hydrogen-bonded O–H bond.

Experimental Section

Spectrometer. The rotational spectrum of the complex was observed in a Fourier-transform microwave spectrometer of the Balle-Flygare type with a modified Bosch fuel injector as a pulsed nozzle source.[11,12] Line widths were typically 20–30 kHz full width at half maximum with partially resolved Doppler doubling. Center frequencies have an estimated

(1) (a) Peterson, K. I.; Klemperer, W. *J. Chem. Phys.* **1984**, *81*, 3842. (b) Peterson, K. I.; Klemperer, W. *J. Chem. Phys.* **1986**, *85*, 725. (c) Yaron, D.; Peterson, K. I.; Zolandz, D.; Klemperer, W.; Lovas, F. J.; Suenram, R. D. *J. Chem. Phys.* **1990**, *92*, 7095. (d) Herbine, P.; Dyke, T. R. *J. Chem. Phys.* **1985**, *83*, 3768. (e) Leung, H. O.; Marshall, M. D.; Suenram, R. D.; Lovas, F. J. *J. Chem. Phys.* **1989**, *90*, 700. (f) Peterson, K. I.; Klemperer, W. *J. Chem. Phys.* **1984**, *80*, 2439.

(2) Hobza, P.; Mulder, F.; Sandorfy, C. *J. Am. Chem. Soc.* **1981**, *103*, 1360.

(3) Barnes, A. J.; Paulson, S. L. *Chem. Phys. Lett.* **1983**, *99*, 326.

(4) (a) Legon, A. C.; Aldrich, P. D.; Flygare, W. H. *J. Am. Chem. Soc.* **1980**, *102*, 7584. (b) Legon, A. C.; Aldrich, P. D.; Flygare, W. H. *J. Am. Chem. Soc.* **1982**, *104*, 1486.

(5) Buxton, L. W.; Aldrich, P. D.; Shea, J. A.; Legon, A. C.; Flygare, W. H. *J. Chem. Phys.* **1981**, *75*, 2681.

(6) (a) Aldrich, P. D.; Kukolich, S. G.; Campbell, E. J.; Read, W. G. *J. Am. Chem. Soc.* **1983**, *105*, 5569. (b) Kukolich, S. G. *J. Chem. Phys.* **1983**, *78*, 3842.

(7) (a) Kukolich, S. G.; Aldrich, P. D.; Read, W. G.; Campbell, E. J. *Chem. Phys. Lett.* **1982**, *90*, 329. (b) Shea, J. A.; Flygare, W. H. *J. Chem. Phys.* **1982**, *76*, 4857. (c) Kukolich, S. G.; Read, W. G.; Aldrich, P. D. *J. Chem. Phys.* **1983**, *78*, 3552.

(8) (a) Legon, A. C.; Aldrich, P. D.; Flygare, W. H. *J. Chem. Phys.* **1981**, *75*, 625. (b) Read, W. G.; Flygare, W. H. *J. Chem. Phys.* **1982**, *76*, 2238. (c) Aldrich, P. D.; Kukolich, S. G.; Campbell, E. J. *J. Chem. Phys.* **1983**, *78*, 3521.

(9) de Meijere, A. *Angew. Chem., Intl. Ed. Engl.* **1979**, *18*, 809 and references therein.

(10) (a) Andrews, A. M.; Taleb-Bendiab, A.; LaBarge, M. S.; Hillig, K. W., II; Kuczkowski, R. L. *J. Chem. Phys.* **1990**, *93*, 7030. (b) Andrews, A. M.; Hillig, K. W., II; Kuczkowski, R. L.; Legon, A. C.; Howard, N. W. *J. Chem. Phys.* **1991**, *94*, 6947. (c) Andrews, A. M.; Hillig, K. W., II; Kuczkowski, R. L. *J. Chem. Phys.* **1992**, *96*, 1784.

(11) Balle, T. J.; Flygare, W. H. *Rev. Sci. Instrum.* **1981**, *52*, 33.

(12) Hillig, K. W., II; Matos, J.; Scioly, A.; Kuczkowski, R. L. *Chem. Phys. Lett.* **1987**, *133*, 359.

0002-7863/92/1514-6765$03.00/0

Table I. Observed Transitions (MHz) and Spectroscopic Constants of $C_3H_6 \cdot H_2O$

	B[a] strong		A[a] weak	
	ν_{obs}	$\nu_o - \nu_c$	ν_{obs}	$\nu_o - \nu_c$
$2_{12}-1_{11}$[b]	9538.013	−0.012	9539.715	−0.015
$2_{02}-1_{01}$	9715.940	−0.002	9717.080	0.002
$2_{11}-1_{10}$	9895.087	0.014	9895.676	0.012
$3_{13}-2_{12}$	14305.798	0.012	14308.359	0.009
$3_{03}-2_{02}$	14570.094	−0.004	14571.827	0.000
$3_{22}-2_{21}$	14571.018	−0.004		
$3_{21}-2_{20}$	14576.470	0.002	14578.252	0.001
$3_{12}-2_{11}$	14841.344	−0.006	14842.236	−0.009
A/MHz	19950 (100)		19945 (160)	
B/MHz	2518.845 (5)		2518.843 (7)	
C/MHz	2340.321 (5)		2340.876 (7)	
D_J/kHz	6.7 (2)		6.7 (3)	
D_{JK}/kHz	189 (1)		184 (4)	
n[c]	8		7	
$\Delta\nu_{rms}$[d]/kHz	8		9	
μ_a/D	1.209 (10)		1.241 (10)	

[a] Symmetry label of the tunneling state. [b] Transition labels are $J'_{K_P'K_O'} - J''_{K_P''K_O''}$. [c] Number of transitions in the fit. [d] $\Delta\nu = \nu_o - \nu_c$.

accuracy of ±4 kHz. For the measurement of Stark effects, the spectrometer is fitted with two steel mesh plates separated by 30 cm to which up to 10 kV can be applied with opposite polarities.

For the resolution of the deuterium nuclear quadrupole hyperfine structure, a new modification of the spectrometer was employed. Following Stahl et al., a nozzle was placed in the center of one of the mirrors of the Fabry-Perot cavity so that the gas jet expanded along the cavity axis.[13] This increased the splitting between components of each Doppler doublet to 60–70 kHz. Furthermore, the combination of reduced transit-time broadening (because the molecules are in the active region of the cavity for a longer time leading to longer free induction decays) and a narrower spread in the velocity distribution on the cavity axis decreased the line width of each component to ~5 kHz, giving much better resolution of the closely spaced hyperfine structure.

Samples. The spectrum of $C_3H_6 \cdot H_2O$ was observed by placing about 1 mL of de-ionized water in a 1-L glass sample bulb. The water was degassed by freezing to liquid nitrogen temperature and pumping for several minutes followed by warming to room temperature; this was repeated for 2 or 3 freeze/thaw cycles until no further gas was evolved. About 10 Torr of C_3H_6 (Aldrich) and 1.5 atm of argon (Linde) were then added to the bulb. The vapor pressure of water at room temperature was sufficient to produce the spectrum with good signal to noise.

Because deuterated water often exchanges with incidental water inside the sample introduction line, the spectra of $C_3H_6 \cdot HDO$ and $C_3H_6 \cdot D_2O$ were observed by placing a 75:25 mixture of D_2O (Cambridge Isotope Labs) and H_2O in a chamber immediately behind the nozzle orifice. A sample containing 1% cyclopropane in argon at 1.5 atm was passed over this solution. The spectra of 1,1-$C_3H_4D_2 \cdot H_2O$, $C_3D_6 \cdot H_2O$, $C_3H_6 \cdot H_2{}^{17}O$, and $C_3H_6 \cdot H_2{}^{18}O$ were produced with the same procedure as the normal isotopic species using commercial samples. No exchange problems were evident between the $H_2{}^{17}O$ or $H_2{}^{18}O$ and water in the sample line. 1,1-$C_3H_4D_2$ (98%), C_3D_6 (>99%), and $H_2{}^{17}O$ (38%) were purchased from MSD Isotopes. $H_2{}^{18}O$ (97%) was obtained from Cambridge Isotope Labs.

Results and Analysis

Spectrum. The spectrum of the $C_3H_6 \cdot H_2O$ complex was predicted with use of a hydrogen-bonded model analogous to $C_2H_4 \cdot H_2O$, and transitions were found in the appropriate region for $J = 2 \leftarrow 1$ *a*-type transitions. This led to predictions for the $J = 3 \leftarrow 2$ transitions of the same series, which were readily found. *b*- and *c*-type Q-branch series were predicted in the 16–18-GHz region, but despite extensive searching no other transitions were found. The observed transitions, listed in Table I, were all split into doublets with a 3:1 relative intensity ratio; in all cases, the lower frequency transition was the more intense. The method by which the relative intensities were determined has been discussed previously.[10a] The strong and weak sets were each fit independently to A, B, C, D_J, and D_{JK} in the Watson S-reduction I^r representation.[14] The fitted constants are shown in Table I. The A rotational constant is poorly determined because the molecule is very prolate ($\kappa = -0.97$) and only *a*-type transitions were observed. Since the split transitions of the spectrum can be fit as two independent states, a high-barrier tunneling process is implied. The 3:1 relative intensities suggest it involves the exchange of the two hydrogen atoms of the water subunit. This will be further discussed below. The symmetry labels A and B are chosen so that the A label corresponds to a spatially symmetric tunneling state which, because of the Fermi–Dirac statistics associated with the interchange of two fermions, is paired to the antisymmetric nuclear spin functions, and the B label corresponds to a spatially antisymmetric tunneling state which is paired to the symmetric nuclear spin functions.[15]

The spectra of $C_3H_6 \cdot HDO$ and $C_3H_6 \cdot D_2O$ were predicted, again using a hydrogen-bonded model, and searches were begun. For $C_3H_6 \cdot D_2O$, the transitions were found split into doublets of unequal intensity. However, where in the normal isotopic species the lower frequency lines were three times as strong as the higher frequency lines, in $C_3H_6 \cdot D_2O$ the higher frequency lines were about two times stronger than the lower frequency transitions. The magnitude of the splittings decreased by about 50–60% for the deuterated form. For $C_3H_6 \cdot HDO$, two different isotopic isomers were expected for a hydrogen-bonded structure, one with the D in the hydrogen bond and the other with the D in the nonbonded position. Only one spectrum was observed and no doubling of the transitions was found. The rotational constants indicated this was the deuterium-bonded isomer. Extensive searches above and below the observed transitions produced no partner and intensive searches for another isomer were not fruitful.

The spectra of $C_3H_6 \cdot H_2{}^{18}O$ and $C_3H_6 \cdot H_2{}^{17}O$ were also split into doublets. For $C_3H_6 \cdot H_2{}^{18}O$ the splitting decreased by 30%. The relative intensities of the two components paralleled the normal isotopic species and were approximately 3:1. $C_3H_6 \cdot H_2{}^{17}O$ also exhibited split transitions with strong and weak components. The ^{17}O nuclear quadrupole hyperfine structure prevented a quantitative determination of their relative intensities.

The spectra of 1,1-$C_3H_4D_2 \cdot H_2O$ and $C_3D_6 \cdot H_2O$ were also measured. For 1,1-$C_3H_4D_2 \cdot H_2O$ two different spectra were observed and both were split into doublets with a 3:1 intensity ratio similar to that of the normal isotopic species. These two spectra correspond to deuteration at the position opposite the C–C bond to which the water is bonded (labeled *apical*) and at one of the carbons in the C–C bond to which the water is bonded (labeled *basal*). The splitting decreased by about 20% for the *apical* position and by about 10% for the *basal* position. The spectrum of $C_3D_6 \cdot H_2O$ was split into doublets with a 3:1 intensity ratio like that of the normal isotopic species, with a decrease in the splitting of about 30%.

The spectroscopic constants for all the isotopically substituted species are shown in Table II. The transition frequencies are available as supplementary material in Table S-I. (See the paragraph at the end of the paper regarding supplementary material.)

Dipole Moment. The dipole moment of the strong B state of $C_3H_6 \cdot H_2O$ was determined by measuring the Stark effects of all 15 $|M|$ components available from the observed transitions. The electric field was calibrated using the $J = 1 \leftarrow 0$, $M = 0 \leftarrow 0$ transition of OCS at 12162.980 MHz.[16] The observed Stark effects of $C_3H_6 \cdot H_2O$, available in Table S-II as supplementary material, were least-squares fit to the dipole components using Stark coefficients calculated from the rigid-rotor rotational constants, resulting in $|\mu_a| = 1.209$ (10) D. The fitted value for $\mu_b{}^2$ was a small negative number (−0.033 D^2) and $\mu_c{}^2$ was 0.021 (68) D^2, implying that $\mu_b \approx \mu_c \approx 0$ D. When the μ_b and μ_c components were constrained to zero, the resulting μ_a component was the same. A similar analysis of the weak state dipole moment resulted in

(13) Stahl, W.; Sutter, D. *Rev. Sci. Instrum.* **1990**, *61*, 3695.

(14) Watson, J. K. G. *Vibrational Spectra and Structure*; Durig, J., Ed.; Marcel Dekker: New York, 1977.

(15) These labels are chosen arbitrarily without attention to a careful permutation–inversion group theoretical analysis.

(16) Tanaka, K.; Ito, H.; Harada, K.; Tanaka, T. *J. Chem. Phys.* **1984**, *80*, 5893.

Table II. Spectroscopic Constants for Cyclopropane–Water Isotopomers (MHz)

	C_3H_6·HDO	C_3H_6·D_2O	C_3H_6·$H_2{}^{18}O$	C_3H_6·$H_2{}^{17}O$	*apical*-$C_3H_4D_2$·H_2O[a]	*basal*-$C_3H_4D_2$·H_2O[b]	C_3D_6·H_2O
		(weak)	(strong)	(strong)[c]	(strong)	(strong)	(strong)
A/MHz	19881 (70)	20000 (500)	19908 (500)	19882 (300)	18676 (100)	16791 (50)	13656 (25)
B/MHz	2492.166 (6)	2388.319 (20)	2361.527 (22)	2436.196 (15)	2351.318 (3)	2496.852 (8)	2315.53 (3)
C/MHz	2317.410 (6)	2226.178 (19)	2203.876 (21)	2268.787 (15)	2211.972 (3)	2306.660 (8)	2152.29 (3)
D_J/kHz	6.5 (3)	5.9 (7)	5.9 (7)	6.1 (5)	5.7 (2)	6.2 (4)	4.7 (9)
D_{JK}/kHz	177 (1)	180 (12)	176 (13)	183 (9)	170 (2)	195 (2)	186 (18)
n	8	6	6	6	7	8	6
$\Delta\nu_{rms}$/kHz	11	9	10	7	4	14	13
		(strong)	(weak)	(weak)[c]	(weak)	(weak)	(weak)
A/MHz		19676 (200)	20422 (500)	19469 (3000)	18633 (130)	16805 (500)	13654 (250)
B/MHz		2388.403 (9)	2361.412 (19)	2436.2 (1)	2351.283 (4)	2496.85 (4)	2315.51 (3)
C/MHz		2226.385 (9)	2204.265 (19)	2269.3 (2)	2212.431 (4)	2307.17 (4)	2152.70 (3)
D_J/kHz		5.2 (3)	6.3 (6)	6.1[d]	5.4 (2)	6.5 (11)	4.7 (9)
D_{JK}/kHz		191 (6)	164 (12)	183[d]	168 (2)	190 (25)	182 (17)
n		6	6	6	7	6	6
$\Delta\nu_{rms}$/kHz		4	9	416	5	18	13

[a] Deuterium at carbon opposite hydrogen bond. [b] Deuterium at carbon adjacent to hydrogen bond. [c] Fit of theoretical unsplit transition frequencies. [d] Fixed at the value determined for stronger species.

Table III. Experimental and Predicted (B + C) and (B − C) for C_3H_6·H_2O in MHz

	exp	hydrogen bonded	bifurcated	stacked
(B + C)	4858	4861	4861	4857
(B − C)	178	167	155	5

$|\mu_a|$ = 1.241 (10) D and $\mu_b \approx \mu_c \approx 0$ D. The dipole moment of C_3H_6·HDO was also measured, giving $|\mu_a|$ = 1.277 (8) D and $\mu_b \approx \mu_c \approx 0$ D.

Nuclear Quadrupole Coupling Constants for C_3H_6·HDO and C_3H_6·$H_2{}^{17}O$. Hyperfine structure arising from deuterium nuclear quadrupole coupling in C_3H_6·HDO was resolved and assigned. The quadrupole interaction was treated as a perturbation on the rotational energy levels, and the coupling constants were derived by least-squares fitting to the observed splittings, resulting in χ_{aa} = 0.242 (3) MHz, χ_{bb} = −0.107 (7) MHz, and χ_{cc} = −0.135 (7) MHz.[17]

For C_3H_6·$H_2{}^{17}O$, the ^{17}O hyperfine structure was assigned for both the strong and weak components of the tunneling doublets. For the strong component a nearly-complete assignment was possible, while for the weaker component only the strongest hyperfine transitions were observed, giving a much smaller data set. The coupling constants were fit as above to give χ_{aa} = −5.352 (10) MHz, χ_{bb} = 2.353 (12) MHz, and χ_{cc} = 2.999 (22) MHz for the stronger transitions and χ_{aa} = −4.8 (2) MHz, χ_{bb} = 2.1 (1) MHz, and χ_{cc} = 2.7 (3) MHz for the weaker transitions. The hyperfine transition frequencies for both the C_3H_6·HDO and C_3H_6·$H_2{}^{17}O$ isotopomers are available in supplementary Tables S-III and S-IV.

Structure. Because the A rotational constants were poorly determined for all isotopomers, only B and C were used in the structure calculations. For isotopic species with split transitions, the constants from the more intense states were used because their A constants were better determined. Since the difference in B and C between the two states is very small, this choice will not markedly affect the structure. It was assumed that the cyclopropane and water structures were unchanged upon complexation.[18,19]

The success of the hydrogen-bonded structural model at predicting the spectra of the normal isotopic species and the isotopomers implied that the complex was likely to be hydrogen bonded or perhaps bifurcated, as the heavy atom positions would be similar for the two structures. Attempts to match the observed B and C rotational constants of the normal isotopic species using the hydrogen-bonded, bifurcated, and stacked models supported this. The results are shown in Table III. The hydrogen-bonded and bifurcated structures, which place the water in the plane of the cyclopropane, result in good matches for $(B + C)$ and $(B - C)$. However, placing the water above the ring in the stacked structure results in a very nearly prolate top with $(B - C) \approx 5$ MHz compared to the observed $(B - C)$ value of 178 MHz.

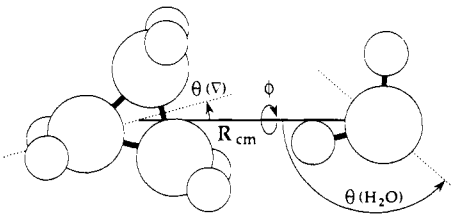

Figure 1. Parameters defining the structure of C_3H_6·H_2O. R_{cm} is the distance between the centers of mass; $\theta(\nabla)$ is the angle between the C_2 axis of cyclopropane and R_{cm}; $\theta(H_2O)$ is the angle between the C_2 axis of H_2O and R_{cm}; ϕ is the torsional angle between the cyclopropane and H_2O planes.

Table IV. Experimental and Predicted Differences in Rotational Constants (MHz) for C_3H_6·H_2O, C_3H_6·HDO, and C_3H_6·D_2O

			bifurcated[d]		hydrogen bonded[e]	
		exp[c]	ϕ = 0°	ϕ = 90°	ϕ = 0°	ϕ = 90°
HDO[a]	ΔB	26	53	59	34	34
	ΔC	23	51	40	29	29
D_2O[b]	ΔB	104	48	54	98	105
	ΔC	91	47	42	81	85

[a] Difference between rotational constants of C_3H_6·H_2O and C_3H_6·HDO. [b] Difference between rotational constants of C_3H_6·HDO and C_3H_6·D_2O. See text for details. [c] Experimental. [d] Calculated for bifurcated structure. [e] Calculated for hydrogen bonded structure.

Once it is established that the heavy atoms all are planar or nearly planar, the geometry of the complex is defined by the parameters shown in Figure 1, where R_{cm} is the distance between the centers of mass of water and cyclopropane, $\theta(H_2O)$ is the angle between the C_2 axis of the water and R_{cm}, $\theta(\nabla)$ is the angle between the C_2 axis of cyclopropane and R_{cm}, and ϕ is the torsional angle between the CCC plane of cyclopropane and the plane of the water (for ϕ = 0° the water hydrogens lie in the cyclopropane CCC plane for either the hydrogen-bonded or bifurcated structures). It is assumed that the out-of-plane tilt angles are negligible compared to model errors arising from vibrational averaging. R_{cm}, defined primarily by the positions of the heavy atoms, can be determined from the moments of inertia of the normal isotopic species to be approximately R_{cm} = 3.7 Å. The inertial data, however, are relatively insensitive to the angles which are defined primarily by the positions of the light hydrogen atoms.

(17) Gordy, W.; Cook, R. L. *Molecular Microwave Spectra*; Wiley: New York, 1984; pp 413–418.
(18) Endo, Y.; Chang, M. C.; Hirota, E. *J. Mol. Spectrosc.* **1987**, *126*, 63.
(19) Heming, D.; DeLucia, F. C.; Gordy, W.; Staab, P. A.; Morgan, H. W. *Phys. Rev. A* **1973**, *5*, 2785.

Table V. Cyclopropane–Water Structures from Least-Squares Fits of Moments of Inertia I_b and I_c

	$\phi = 0°$	$\phi = 90°$
$\theta(H_2O)$/deg[a]	124.8 (4.0)	123.0 (6.3)
R_{cm}/Å[a]	3.712 (1)	3.713 (2)
$(I_{obs} - I_{calc})_{rms}$/amu·Å^2	0.45	0.67
$R_{H\text{-}bond}$/Å[b]	2.342	2.343
$\theta_{H\text{-}bond}$/deg[b]	3	4

[a] Fitted parameters. [b] Calculated parameters (not explicitly fit). $R_{H\text{-}bond}$ is the distance from the hydrogen-bonded H to the C–C bond center. $\theta_{H\text{-}bond}$ is the deviation from 180° of the angle subtended by the C–C bond center, the hydrogen-bonded H, and the O.

The angle $\theta(H_2O)$ can be approximated from the moments of inertia of C_3H_6·HDO and C_3H_6·D_2O. The measured changes in rotational constants upon deuteration, $\Delta B(HDO) = B(C_3H_6\cdot H_2O) - B(C_3H_6\cdot HDO)$ and $\Delta B(D_2O) = B(C_3H_6\cdot HDO) - B(C_3H_6\cdot D_2O)$, are shown in Table IV. The small change upon substitution of one deuterium followed by the large change for the second suggests that the two water hydrogens are in significantly different positions. To test this inference R_{cm} was adjusted for the bifurcated ($\theta(H_2O) = 0°$) and linear hydrogen-bonded ($\theta(H_2O) = 126°$) structures to best match B and C for $C_3H_6\cdot H_2O$. From these structures, changes in the B and C rotational constants were predicted for the two deuterated water isotopes for both $\phi = 0°$ and 90°. Regardless of the angle ϕ, the agreement was very poor for the bifurcated structure and quite good for the hydrogen-bonded structure. Although the A constants were poorly determined, Kraitchman's equations can be used to calculate the a coordinates of the water hydrogens to within ±0.15 Å.[20] First the normal isotopic species was used as the parent to calculate the position of the deuterium in C_3H_6·HDO, and then C_3H_6·HDO was used as the parent to calculate the position of the second deuterium in $C_3H_6\cdot D_2O$. This calculation provided qualitative agreement, in that the a coordinate was small for the first hydrogen atom (1.46 Å) and large for the second (2.97 Å), consistent with the hydrogen-bonded structure where the C_3H_6·HDO species is deuterium bonded.

The angle $\theta(H_2O)$ above was determined independently of the angle $\theta(\nabla)$. This is possible because cyclopropane, a symmetric top molecule, may be rotated by any angle about its local C_3 axis without affecting the moments of inertia of the normal isotopic species of the complex. The orientation of the cyclopropane can be determined from the 1,1-$C_3H_4D_2\cdot H_2O$ isotopic species. The similarity of P_{bb} of $C_3H_6\cdot H_2O$ (20.3592 amu·Å^2) to P_{bb} of *apical*-$C_3H_4D_2\cdot H_2O$ (20.2998 amu·Å^2) places the substituted hydrogens in or nearly in the ac plane of the complex and requires that $\theta(\nabla)$ be approximately zero.

The torsional angle ϕ is not readily determined from the moments of inertia. It is defined primarily by the b and c coordinates of the nonbonded hydrogen atom on the water. The moments of inertia, being subject to vibrational averaging effects of the same magnitude as the inertial contributions from the b and c coordinates of a hydrogen atom, are not reliable indicators of these coordinates.[21] All the experimental data were fit to R_{cm} and $\theta(H_2O)$ for $\phi = 0°$ (nonbonded H in the CCC plane) and $\phi = 90°$ (nonbonded H perpendicular to the CCC plane). The results are shown in Table V. Although the quality of the fit is slightly better for $\phi = 0°$, the difference is too small to be conclusive.

In summary, the structure of $C_3H_6\cdot H_2O$ is determined from the inertial data to be hydrogen bonded with an approximately linear hydrogen bond, as measured by the angle between the C–C bond center, the bonded hydrogen atom, and the oxygen atom (Table V). The position of the free hydrogen atom on the water is ambiguous. Such a structure leaves two puzzling observations. The first is that the observed dipole moment is not consistent with a hydrogen-bonded structure. If the dipole moment of water[19] is projected onto the principal axis system of the complex, components $\mu_a = 1.15$ D and $\mu_\perp = 1.45$ D are expected, where $\mu_\perp = [\mu_b^2 + \mu_c^2]^{0.5}$. The experimentally measured components are $\mu_b \approx \mu_c \approx 0$ D. The second puzzle is that the ^{17}O quadrupole coupling constants χ_{bb} and χ_{cc} are also quite different from those predicted by a projection of the $H_2{}^{17}O$ nuclear quadrupole coupling tensor onto the principal axis system of the complex.[22] These values are listed in Table VI as "predicted (rigid)". For completeness, predicted and observed deuterium quadrupole coupling constants for C_3H_6·HDO, which do not exhibit such a discrepancy, are also included in Table VI.

Table VI. Dipole Moment Components, ^{17}O and Deuterium Nuclear Quadrupole Coupling Constants Predicted from the Structure, and Experimental Values[a]

	predicted[b] (rigid)	predicted[c] (free rotor)	obsd
μ_a/D	1.15	1.15	1.209 (2)
$\mu_\perp$/D	1.45	0.0	0.0
^{17}O			
χ_{aa}/MHz	−6.039	−6.039	−5.342 (10)
χ_{bb}[d]/MHz	−4.129	3.020	2.356 (12)
χ_{cc}[d]/MHz	10.169	3.020	2.986 (22)
HDO			
χ_{aa}/MHz	0.308	0.308	0.242
χ_{bb}[d]/MHz	−0.133	−0.154	−0.107
χ_{cc}[d]/MHz	−0.175	−0.154	−0.135

[a] Experimental values are as measured for the B tunneling state. [b] Predicted for a rigid molecule with structure as determined from moments of inertia. [c] Predicted assuming the structure determined from the moments of inertia and a free internal rotation of the water subunit about the O–H bond. [d] χ_{bb} and χ_{cc} are for the $\phi = 0°$ structure. The predicted values will be reversed for the $\phi = 90°$ structure.

The most plausible explanation for the dipole moment and quadrupole coupling constant discrepancies is that the water subunit is involved in a free or nearly free internal rotation about the hydrogen-bonded O–H bond and that the observed transitions belong to the cylindrically-symmetric $m = 0$ state. For a nearly free rotor, where the top can be thought of as classically rotating rather than tunneling, both the dipole moment and the nuclear quadrupole coupling constants would be averaged over the tunneling coordinate, reducing $\langle\mu_\perp\rangle$ and giving $\langle\chi_{bb}\rangle$ and $\langle\chi_{cc}\rangle$ values between the predicted χ_{bb} and χ_{cc}, similar to what is observed. The values expected for a cylindrically distributed $m = 0$ state are listed in Table VI as "predicted (free rotor)".

Finally, if it is assumed that the C_3H_6·HDO quadrupole coupling tensor, which is nearly cylindrically symmetric about the O–D bond for free HDO, is cylindrically distributed about the O–D bond by the internal rotation, the averaging angle from zero-point oscillations can be calculated by appropriate rotation of the tensor axis system. This results in $\arccos\langle\cos^2\alpha\rangle^{0.5} = 12°$ for the average angle the O–D bond makes with the a axis in the ab plane of the complex (i.e the bending angle in the CCC plane). Similarly, $\arccos\langle\cos^2\beta\rangle^{0.5} = 19°$ for the angle relative to the a axis in the ac plane (i.e. the out-of-plane bend).

Origin of Tunneling Doublets. We have considered whether the observed splittings in the spectrum arise from the internal rotation described in the previous section or from a high-barrier process which interchanges the hydrogen-bonded and the free hydrogen atoms as was suggested in the Spectrum section above. There are several indications that the split transitions do not originate from the ground state and a nearly free rotor excited state. The approximately 3:1 relative intensities and second-order Stark effects for both states are not consistent with this possibility. It also seems unlikely that the doublets arise from a ground and excited state due to tunneling through a high-barrier internal rotation about the hydrogen-bonded O–H axis. This would not lead to the dipole moment and quadrupole coupling constant averaging discussed in the previous section. Moreover, the observation of singlets for the C_3H_6·HDO species is inconsistent with the doubling arising from either a high-barrier or low-barrier

(20) Kraitchman, J. *Am. J. Phys.* **1953**, *21*, 17.

(21) Because of the large error in the A rotational constant, the Kraitchman calculation does not determine the angle ϕ. For errors of ±500 MHz in A, the b and c coordinates of the free hydrogen atom range from 0.1 to 0.8 Å.

(22) Garrey, R. M.; DeLucia, F. C. *Can. J. Phys.* **1977**, *55*, 1115.

Table VII. Relative Intensities[a] of B:A Tunneling States for $C_3H_6 \cdot H_2O$ and Isotopomers

$C_3H_6 \cdot H_2O$	2.6:1
$C_3H_6 \cdot HDO$	*b*
$C_3H_6 \cdot D_2O$	(1:2)
$C_3H_6 \cdot H_2{}^{18}O$	(3:1)
$C_3H_6 \cdot H_2{}^{17}O$	(3:1)
$C_3D_6 \cdot H_2O$	(3:1)
apical-1,1-$C_3H_4D_2 \cdot H_2O$	2.8:1
basal-1,1-$C_3H_4D_2 \cdot H_2O$	2.9:1

[a] Relative intensities measured as described in ref 10a. Uncertainties are about 15%. Numbers in parentheses are estimated. [b] Only one set of transitions observed.

internal rotation tunneling about the O–H bond.

Evidence that the doublets arise from a tunneling process involving the exchange of the water hydrogens is found in the intensity behavior for various isotopic species. The 3:1 relative intensities of the B and A states in the normal isotopic species are suggestive of a tunneling path which exchanges these two hydrogen atoms. This is confirmed by the relative intensities of the two states in the other isotopomers shown in Table VII. For $C_3H_6 \cdot D_2O$ the relative intensities reverse for the two states, consistent with the 1:2 nuclear spin statistical weights for the exchange of two deuterons. The lack of tunneling splittings in the $C_3H_6 \cdot HDO$ suggests that the tunneling motion involves the exchange of the two water hydrogens and that they are in two inequivalent positions in the complex. Additionally, *apical*-$C_3H_4D_2 \cdot H_2O$, *basal*-$C_3H_4D_2 \cdot H_2O$, and $C_3D_6 \cdot H_2O$ all exhibit the same 3:1 relative intensities observed in the normal isotopic species, indicating that the cyclopropane does not exchange its protons in the tunneling motion. These considerations eliminate all tunneling paths except those which permute the two water protons and only the two water protons as the source of the doubling.

This permutation of the two protons on the water can be accomplished through a number of pathways. The two most likely are the rotation of the water subunit about its C_2 symmetry axis (its molecular *b* axis) or the rotation of the water about an axis perpendicular to its molecular plane (its molecular *c* axis) which is coupled to the free rotation about the O–H bond discussed above. Alternatively this can be thought of as an interchange of the water hydrogens through a bifurcated intermediate coupled with a rotation of the cyclopropane about the hydrogen bond axis. These are illustrated in Figure 2, where the end result of Pathway 1 is equivalent to that of Pathway 2 by a simple overall rotation of the complex by 180°. Several factors favor Pathway 2. The first and most compelling is the difference in the μ_a dipole moment for the two tunneling states, where μ_a for the spatially symmetric state is 1.241 D and μ_a for the spatially antisymmetric state is 1.209 D. The rotation of water about its local C_2 symmetry axis should have no effect on the dipole moment. This is not the case for rotation about its *c* inertial axis. As discussed by Yaron et al., regarding the H_2O-CO spectrum, the symmetric tunneling state wave function is larger at the top of the barrier than the antisymmetric state wave function, which has a node at the barrier.[1c] This argues for the rotation about the *c* inertial axis with a bifurcated intermediate which has the water hydrogens pointed toward the cyclopropane leading to a slightly larger average dipole moment for the symmetric tunneling state. Further, it appears that this pathway may be energetically favored. This route never fully breaks the hydrogen bond connection, but rather it proceeds via a favorable bifurcated intermediate. The rotation about the C_2 axis, however, requires greater severance of the hydrogen bond. Also, the complex sensitivity of the tunneling splitting with isotopic substitution in cyclopropane and water seems consistent with a coupled exchange–rotation pathway, rather than a simple rotation of the water about its C_2 symmetry axis, where the splitting should be primarily affected by substitution on the water.

Finally, the lack of additional excited states from the free or near free internal rotation motion can be attributed to the low rotational temperature (~1 K) of the jet and the effective relaxation of both nuclear spin states into one of the two lowest proton tunneling states with different spatial symmetries.

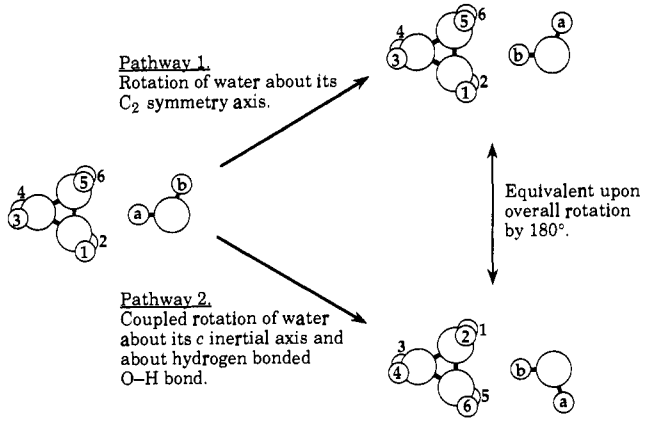

Figure 2. Two likely pathways for the interchange of the water protons (labeled a and b). Pathway 1 represents the rotation of the water subunit about its local C_2 symmetry axis. Pathway 2 represents the rotation of the water subunit about its *c* inertial axis (perpendicular to the water plane) coupled to the rotation of the water about its O–H bond. The end results of the two pathways are equivalent to one another through an overall rotation of the complex by 180°. Note: This figure is drawn for convenience to illustrate the pathways and should not imply that the position of the non-hydrogen bonded hydrogen atom of the water is as shown. The spectrum is consistent with a random orientation for this atom.

Discussion

Following the pattern of the related complexes (e.g. $C_3H_6 \cdot HX$, $C_2H_4 \cdot HX$, $C_2H_2 \cdot HX$, and $C_2H_4 \cdot H_2O$), the $C_3H_6 \cdot H_2O$ complex has the H_2O hydrogen bonded to a C–C edge which behaves as a pseudo-π system hydrogen bond acceptor. This is not in agreement with the previous matrix IR and ab initio studies. It should be noted, however, that the structure of a complex observed in a matrix-isolation experiment is often considerably different from the structure of the complex in the gas phase. A classic example of this is the water dimer, where the complex is hydrogen bonded in the gas phase, but matrix IR work indicates a bifurcated structure.[23] With regard to the theoretical results, the experimental gas-phase structure was not among the structures considered in the calculations so the lack of agreement is not surprising.

To examine whether ab initio theory could be used to correctly predict the structure of the $C_3H_6 \cdot H_2O$ complex, energy minimization calculations were carried out for the stacked, bifurcated and hydrogen-bonded models using the GAUSSIAN86 program package.[24] The calculations were done at the Hartree–Fock level using a 6-31G* basis set and the monomers were held rigid at their free gas-phase geometries. For the hydrogen-bonded and bifurcated structures the energy was minimized with respect to R_{cm} for both the $\phi = 0°$ and 90° structures. In the case of the hydrogen-bonded model $\theta(H_2O)$ was also varied. The stacked structure was assumed to have C_s symmetry and energy was minimized with respect to R_{cm}. The energy of dimerization (ΔE) was calculated by subtracting the energies calculated for the C_3H_6 and H_2O monomers from the total energy calculated for the $C_3H_6 \cdot H_2O$ complex for each model. These calculations are not sophisticated in that they do not take into account configuration interaction and basis set superposition error which are important in calculating reliable energies for weak complexes.[25] Despite this, our laboratory has had considerable success at duplicating the general features of experimental structures using calculations of this level; examples include ethylene·SO_2,[10a] acetylene·SO_2,[10b]

(23) (a) Hagen, W.; Tielens, A. G. G. W. *J. Chem. Phys.* **1981**, *75*, 4198. (b) Dyke, T. R.; Mack, K. M.; Muenter, J. S. *J. Chem. Phys.* **1977**, *66*, 498.
(24) Frisch, J. M.; Binkley, J. S.; Schlegel, H. B.; Raghavachan, K.; Melius, C. F.; Martin, R. L.; Stewart, J. J. P.; Bobrowicz, F. W.; Rohlfing, C. M.; Kahn, L. R.; DeFrees, D. J.; Whiteside, R. A.; Fox, F. J.; Fluder, E. M.; Pople, J. A. GAUSSIAN86; Carnegie-Mellon Quantum Chemistry Publishing Unit: Pittsburgh, PA, 1986.
(25) van Lanthe, J. H.; van Dam, T.; van Duijneveldt, F. B.; krom-Batenberg, L. J. M. *Faraday Symp. Chem. Soc.* **1984**, *19*, 125.

Table VIII. Results of ab Initio Calculations[a] for $C_3H_6 \cdot H_2O$

	H bonded		bifurcated		
	$\phi = 0°$	$\phi = 90°$	$\phi = 0°$	$\phi = 90°$	stacked
R_{cm}/Å	3.94	3.93	2.96	3.02	3.614
$\theta(H_2O)$/deg	126	129			
$-\Delta E^b$/cm^{-1}	405	398	76	32	330

[a] Calculations were done using GAUSSIAN86 at the Hartree–Fock level with a 6-31G* basis set. [b] ΔE is calculated as the total energy of $C_3H_6 \cdot H_2O$ less the energy of C_3H_6 and H_2O.

cyclopropane·SO_2,[10c] trimethylamine·SO_2,[26] dimethylamine·SO_2,[27] dimethyl ether·SO_2[28] and water·SO_2.[28]

The ab initio results are shown in Table VIII; the total energies calculated in each case are given in ref 29. The first observation is that the theoretical results indicate that all of the structural models represent bonded configurations (i.e. have a negative ΔE of dimerization). The hydrogen-bonded structure is the most stable, followed by the stacked (70 cm^{-1} higher in energy) and the bifurcated structures (>300 cm^{-1} higher in energy). Second, for the hydrogen-bonded model the ab initio structural parameters R_{cm} and $\theta(H_2O)$ are in reasonable agreement with the experimental values; $\theta(H_2O)$ is within a few degrees of the fitted value in Table VI with a nearly linear hydrogen bond, although the R_{cm} distance is predicted to be about 0.2 Å too long. Third, the small difference in ΔE between the $\phi = 0°$ and 90° structures supports the hypothesis that the complex has a low barrier to internal rotation about the O–H bond.

The question was raised in the introduction whether the anesthetic properties of cyclopropane could be attributed to the interruption of hydrogen bonding. While this study does not directly address this issue, a comparison of the binding energy of the cyclopropane–water complex with that of other complexes which model biological interactions can shed some light on whether hydrogen bonding to cyclopropane is a significant competitor with hydrogen bonding to O—H, N—H, and C=O groups. With use of Millen's modified pseudodiatomic model, the stretching force constant for the cyclopropane–water hydrogen bond is calculated as 0.065 mdyn/Å.[30] With a Lennard-Jones 6–12 potential this gives a binding energy of 731 cm^{-1} or 2.1 kcal/mol. Binding energies estimated in this manner for electrostatically-dominated interactions are not highly accurate but are useful as a relative gauge of interaction strengths. With the use of the same pseudodiatomic model, binding energies for the water dimer[23b] and formamide–water[31] complexes are calculated as about 2.1 and 4.7 kcal/mol, respectively. It appears that cyclopropane–water interactions would effectively compete for binding sites with water–water interactions. The formamide–water value is about twice as large as the binding energy of cyclopropane–water. Nevertheless, for high concentrations of cyclopropane, the cyclopropane–water complex would be present in significant amounts in an equilibrium situation.

Finally, the cyclopropane–water complex may be compared to the related ethylene–water and acetylene–water complexes. The hydrogen-bonded structure is very similar to that observed in ethylene–water, with the hydrogen bond somewhat shorter in the cyclopropane–water complex (2.34 Å versus 2.48 Å). A similar difference in hydrogen bond length has been observed in complexes of cyclopropane and ethylene with SO_2,[10] HCl,[4] HF,[5] and HCN.[6] Our interpretation of the internal dynamics of the cyclopropane–water complex is that the water subunit is involved in two internal motions: the first is a free or nearly free rotation about the hydrogen-bonded O–H bond which manifests itself in anomalous dipole moment components and ^{17}O quadrupole coupling constants; the second is a high-barrier in-plane wagging motion about the c inertial axis of water coupled to the above motion which interchanges hydrogens and results in doubling of the rotational transitions. This differs from the interpretation of the ethylene–water spectrum where a similar splitting was attributed to the high-barrier internal rotation of the water subunit about the hydrogen-bonded O–H bond.[1a] This investigation, however, was limited to the normal isotopic form and the $C_2H_4 \cdot D_2O$ isotopomer. We are currently reinvestigating the ethylene–water spectrum and examining several other isotopomers in an attempt to understand this difference.

Acknowledgment. This work was funded by a grant from the National Science Foundation. A.M.A acknowledges the support of a Regents-Baer Fellowship at the University of Michigan. Several helpful suggestions from Dr. Amine Taleb-Bendiab are gratefully acknowledged.

Supplementary Material Available: Tables of observed transition frequencies for isotopomers, Stark effect data, and nuclear quadrupole hyperfine splittings (4 pages). Ordering information is given on any current masthead page.

(26) Oh, J.-J.; LaBarge, M. S.; Matos, J.; Kampf, J. W.; Hillig, K. W., II; Kuczkowski, R. L. *J. Am. Chem. Soc.* **1991**, *113*, 4732.
(27) Oh, J.-J.; Hillig, K. W., II; Kuczkowski, R. L. *J. Phys. Chem.* **1991**, *95*, 7211.
(28) Oh, J.-J.; Hillig, K. W., II; Kuczkowski, R. L. *Inorg. Chem.* **1991**, *30*, 4583.
(29) Total energies (hartrees) from Gaussian calculation are as follows: $C_3H_6 \cdot H_2O$ complex hydrogen-bonded ($\phi = 0°$), −193.065500; hydrogen-bonded ($\phi = 90°$), −193.0654699; bifurcated ($\phi = 0°$), −193.0640043; bifurcated ($\phi = 90°$), −193.0638; stacked, −193.0651634; cyclopropane monomer, −117.0566657; water monomer, −76.0069904.
(30) Millen, D. J. *Can. J. Chem.* **1985**, *63*, 1477.
(31) Lovas, F. J.; Suenram, R. D.; Fraser, G. T.; Gillies, C. W.; Zozom, J. *J. Chem. Phys.* **1988**, *88*, 722.